

Discovery and investigation of new eclipsing variable star HD 182144

Krushevskia Viktoriia^{1,2}, Marsakova Vladyslava³, Shugarov Sergey¹

Illia Garbzhii-Romanchenko³, Ivan Andronov⁴, Mykyta Bilodid⁵

¹ *Astronomical Institute of the Slovak Academy of Sciences, Tatranska Lomnica, Slovakia*

² *Main astronomical observatory of National Academy of Sciences of Ukraine, Kyiv, Ukraine*

³ *Odesa Richelieu Science lyceum, Odessa, Ukraine*

⁴ *Odesa National Maritime University*

⁵ *Taras Shevchenko National University of Kyiv*

HD182144

During the processing and analysis of photometric observations for 2018 in the field of symbiotic star CH Cyg we found that one of the comparison stars, namely HD182144, exhibits Algol-like variability.

Tab. 1. Simbad data for HD182144

ICRS coord. (<i>ep=J2000</i>)	19 20 55.48 +49 26 23.49
Gal coord. (<i>ep=J2000</i>)	080.851676351 +15.793425324
Parallax (<i>mas</i>):	2.1074 [0.0155]
Spectral type	A
Fluxes	B 9.16 [0.02] V 9.08 [0.02] G 9.0534 [0.0028] J 8.820 [0.026] H 8.795 [0.030] K 8.753 [0.021]

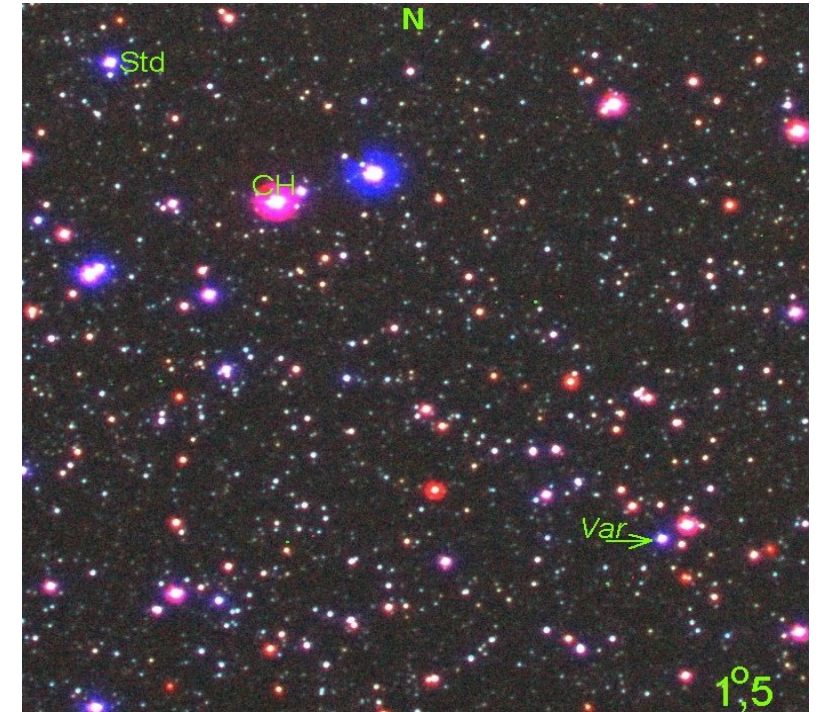


Fig.1. Color map of Variable star field

We checked if this variable is not already known. After comparing with the databases of the General Catalog of Variable Stars and AAVSO, the International Variable Star Index, it turned out that this star is not listed in their bases.

Observations

- In 2023 we provide new $UBVR_cI_c$ -photometric observations, as well as the processing of archival (obtained in 2018, B -band) observations of the selected field, carried out on Zeiss-600 cassegrain telescope and 60\180 mm photolens in AI SAS, Tatranska Lomnica, Slovakia.
- There were 50 observation nights in total. Exposure time ranged from 5 to 10 seconds for Zeiss-600 and from 30 to 90 seconds for photolens, depending on the filter and weather conditions.
- We performed the aperture photometry of our data using the MaxIM DL4+DSLR software package. The star HD 183254 (Sp. type A1) was taken as a comparison star. Standard procedure (dark and flat field correction) was done.

Results

We processed our data for 2018 and 2023 and analyzed it using the WINEFK variability search program. It was confirmed that the variable is an eclipsing binary of detached components. From the resulting periodogram shown in Figure 2, we estimated the orbital period as

$$P = 6.5124 \text{ days}$$

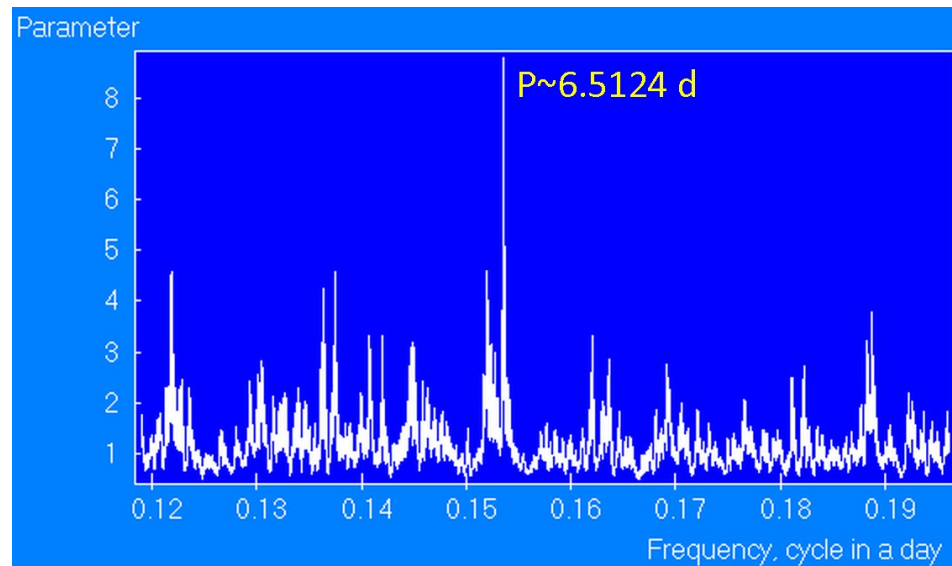


Fig. 2. Obtained periodogram

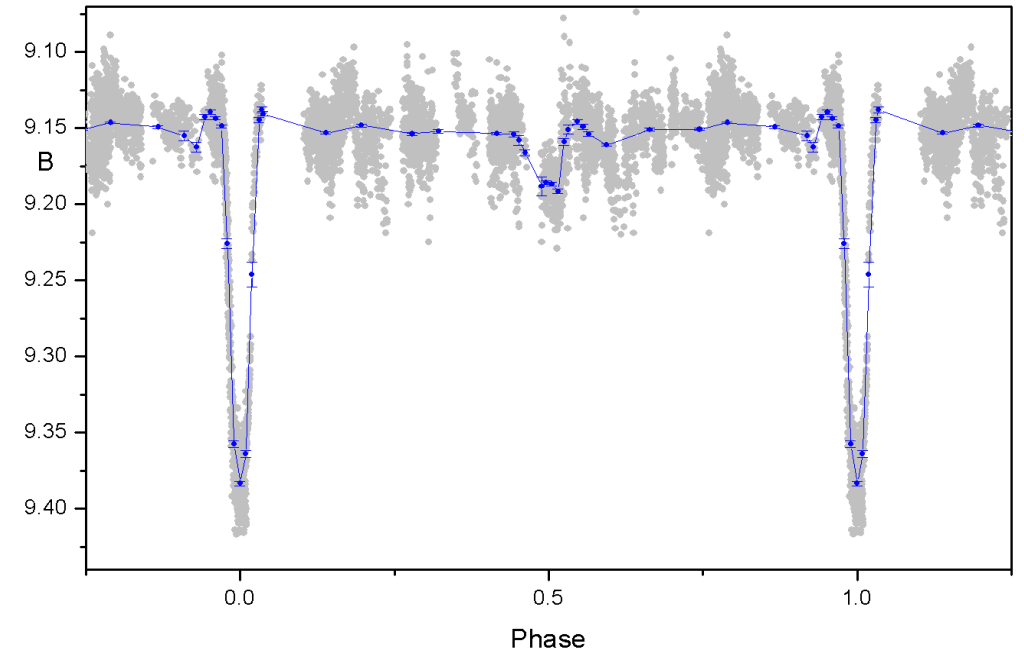


Fig. 3. Folded phase curve in *B*-band (data from 2018 and 2023)

Magnitudes and color indices

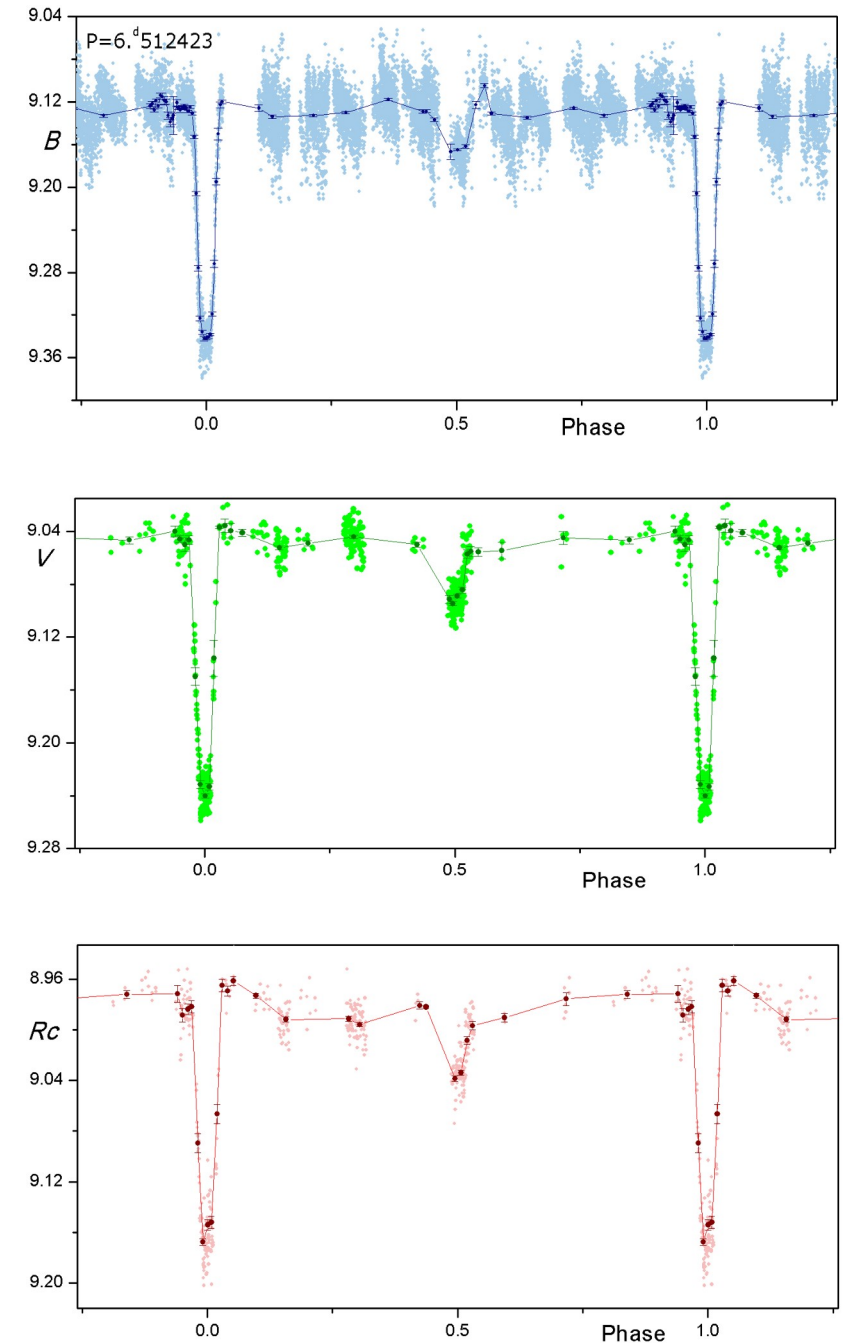
We constructed phase folded curves for B , V and R_C filters on 2023 data. Figure 4 shows the change in depths of the minima, depending on the observation band.

We found average magnitudes for primary and secondary minima and outside the eclipse. This allowed us to determine the corresponding color indices $B-V$, $V-R_C$. Their values are given in Table 2.

Tab.2. Calculated magnitudes and color indices

	B	V	R_C	$B-V$	$V-R_C$
MinI	9.35	9.24	9.175	0.11	0.065
MinII	9.16	9.09	9.04	0.07	0.05
Max	9.12	9.04	8.985	0.08	0.055

Fig. 4. Folded phase curves in B, V, R - bands (data from 2023)



Photoplates from Sonneberg Observatory

We measured 260 archive photoplates from Sonneberg Observatory collection (exposed in 1956-1995).

We folded the obtained magnitudes with the period found above (Fig.5).

Further to construct the O - C curve we used all these measurements near Minimum I and with magnitudes fainter than 9.38 (indicated in red). We take the error estimates for time of these points to be about ± 1 hour.

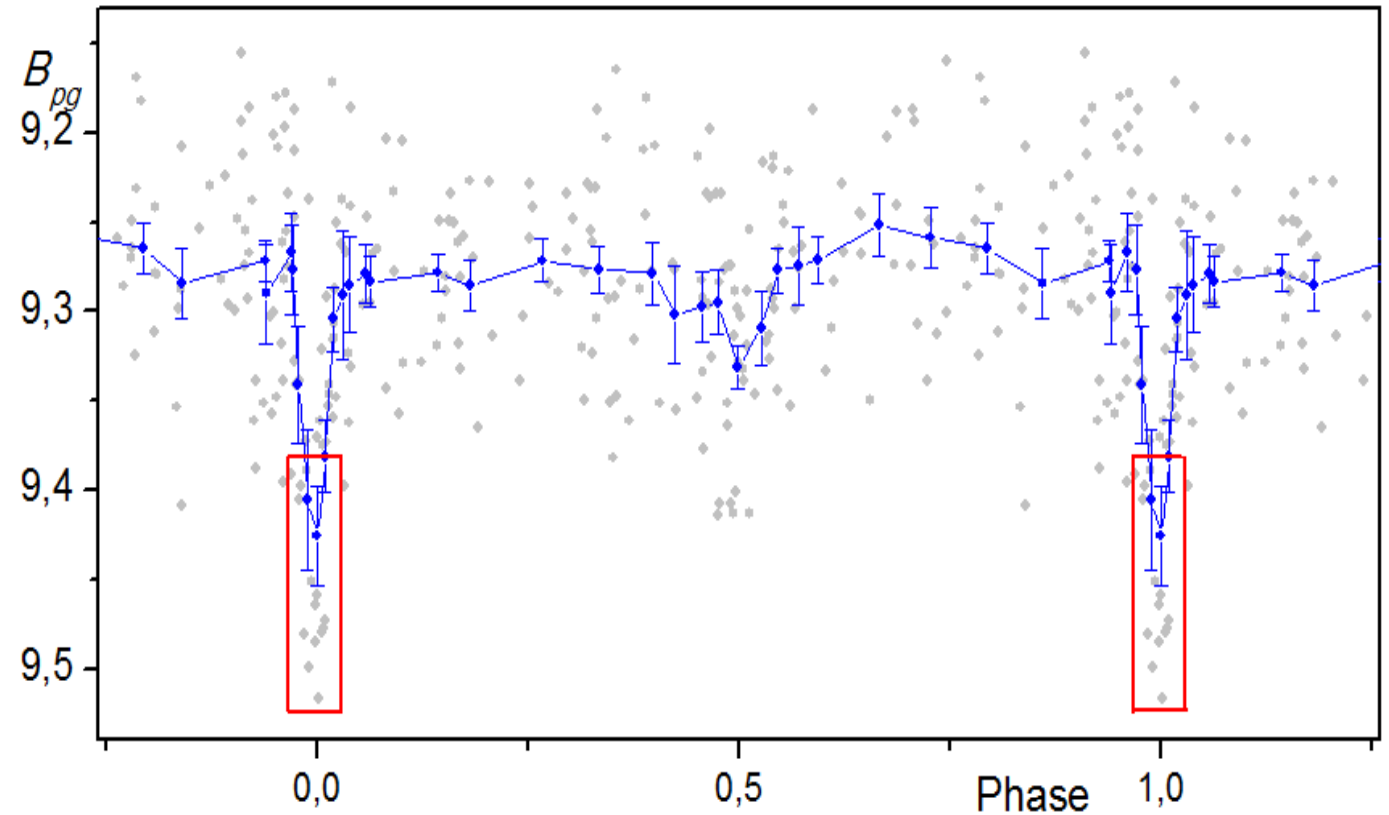


Fig. 5. Phase curve for measurements by using Sonneberg Observatory collection.

TESS Observations

We used and analyzed data obtained from TESS satellite (2021 and 2022).

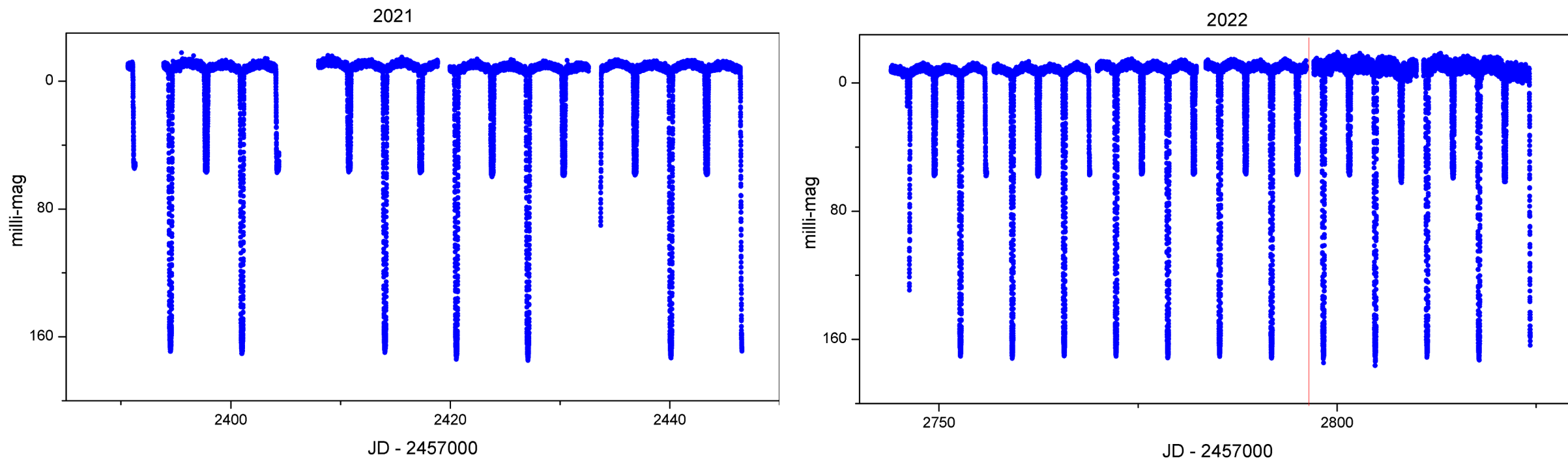


Fig. 6. TESS observations

Approximation of the minima (TESS)

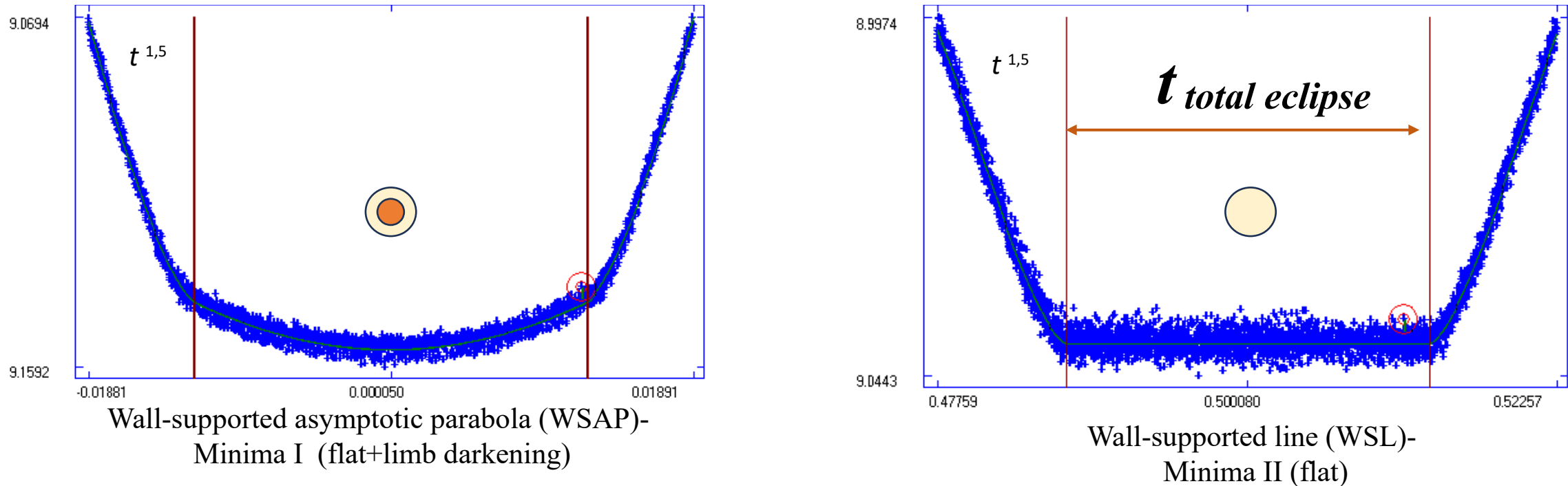


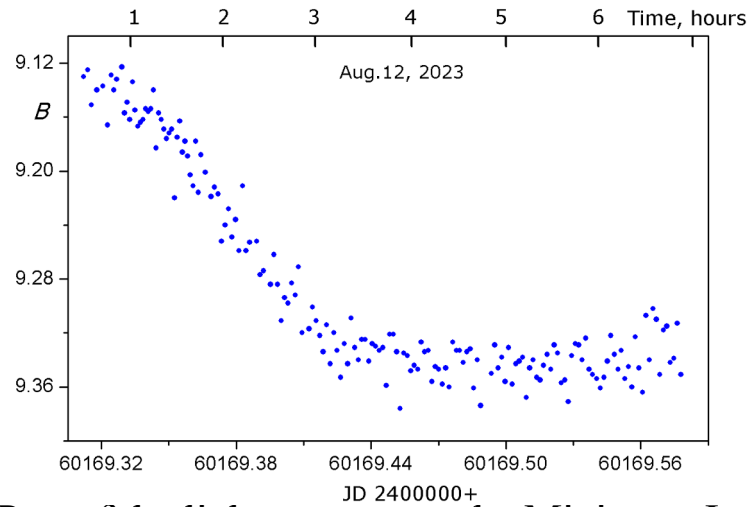
Fig. 7. Approximation of I and II minima from TESS data

From the resulting shape of the secondary minimum (Min.2), namely its flat part, we can conclude that there is a total eclipse of one component by the other.

To determine the exact moments of eclipse minima obtained from TESS data, we used the MAVKA program.

MAVKA –
Andrych, Andronov, Chinarova, 2020,
Journal of Physical Studies 24(1), Article 1902

Minima (AI SAS, 2023)



Part of the light curve near the Minimum I.

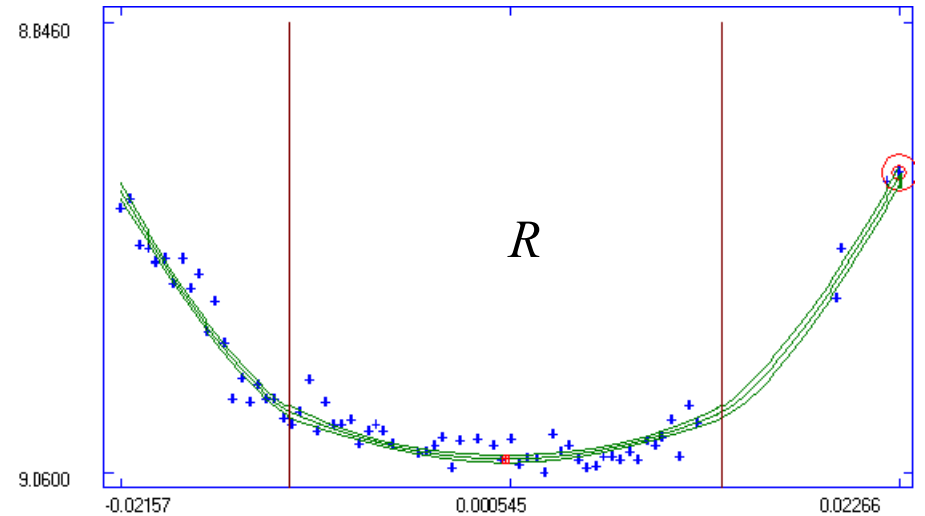
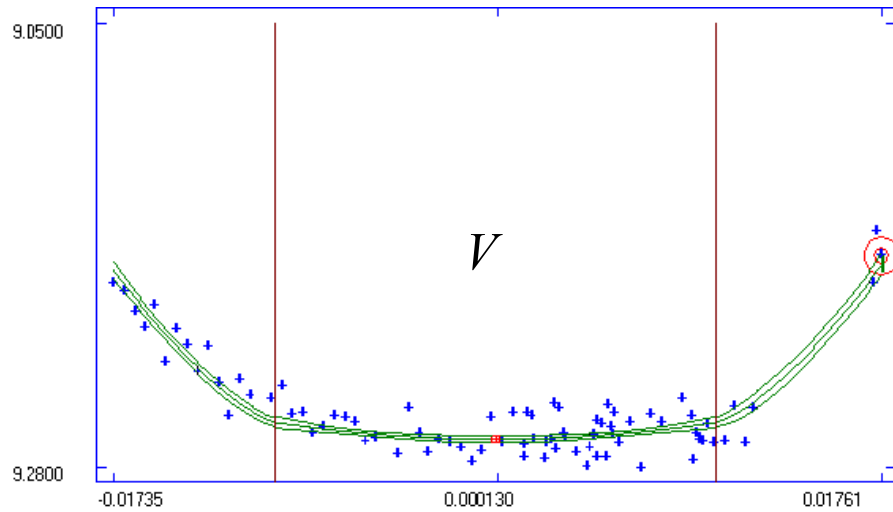
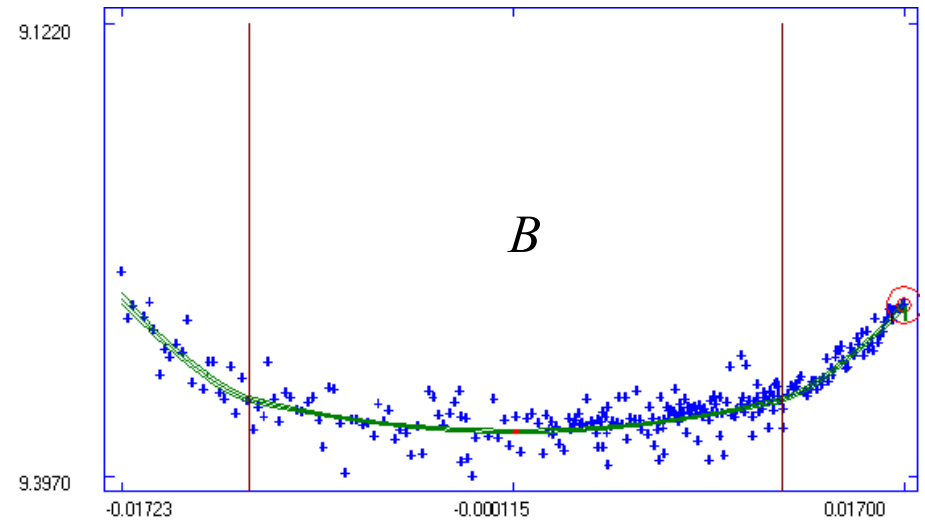


Fig. 8. Wall-supported asymptotic parabola (WSAP) method for Minima I.

Orbital period improvement using O-C method

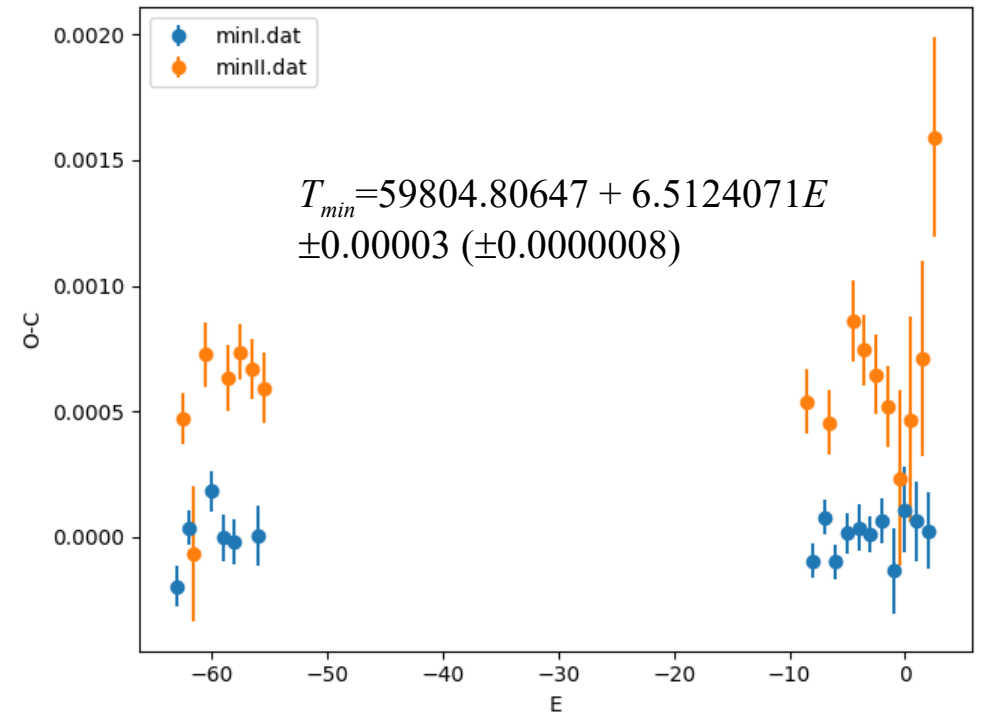
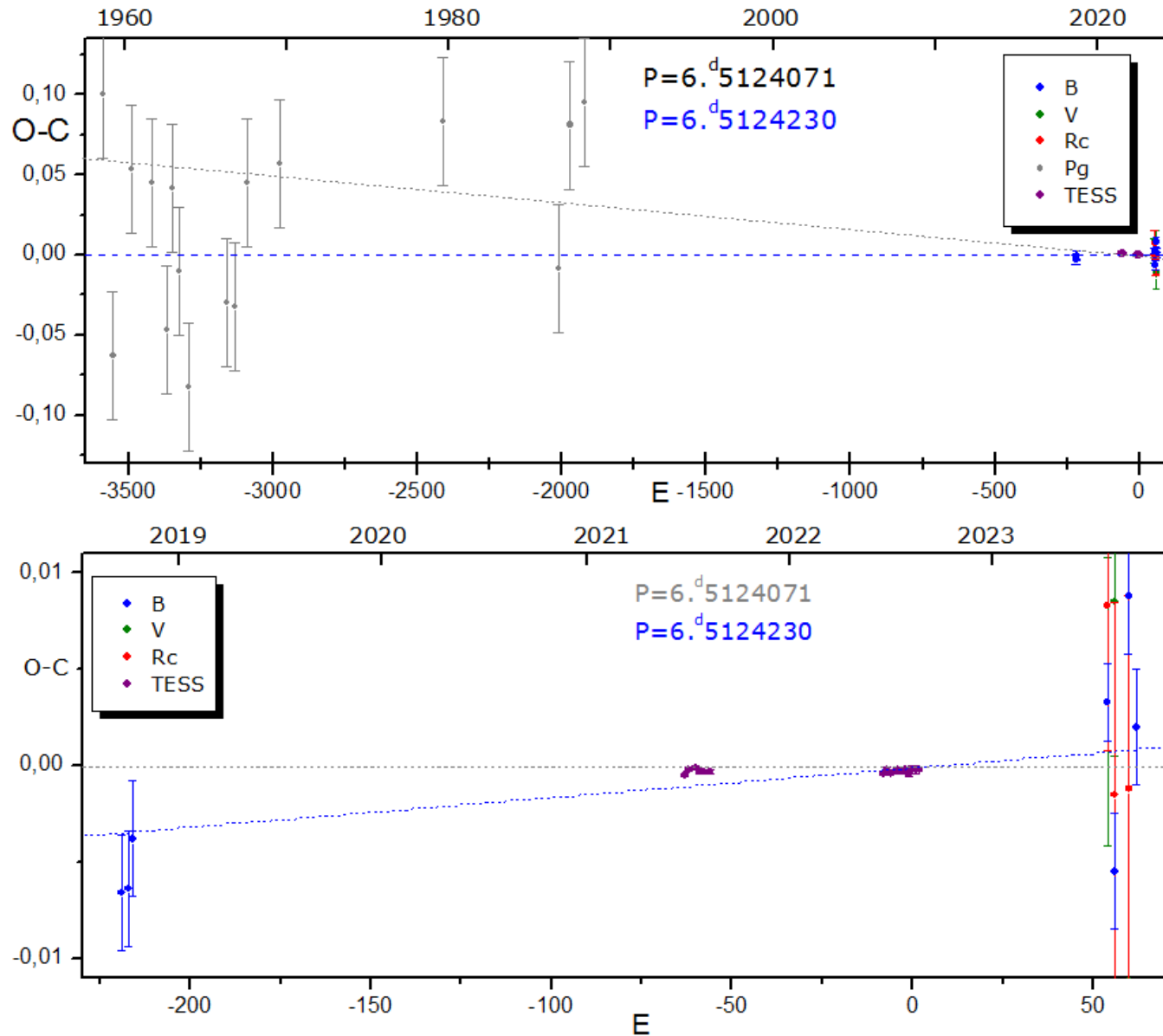


Fig. 9. O - C diagrams: left – only for Minimum I, right – for both minima.

Two-color diagram

Fig. 10 shows the position of the variable on the V-R/B-V diagram in phases corresponding to both minima and the out-of-eclipse part. The original positions taken from Table 2 are plotted in red symbols, and the same phases, but corrected for the value of interstellar reddening, are plotted in blue symbols.

The color excess $E(B-V) = 0.093$ was taken from APOGEE-2 catalog (2022ApJS,259,35A).

The distance to the system, found from the trigonometric parallax (from Table 1):

$$d = 475 \text{ pc.}$$

According to the formula $m_V - M_V = 5 \lg d - 5 - A_V$,
where $A_V = 3.1E(B-V)$,

we calculate that the absolute magnitude of the primary component is $M_V = 0^m.415$.

This value corresponds to a star \sim B9-A0V located on the Main Sequence.

So from the position of the primary and secondary minima, it can be concluded that the system consists of a bright and hot component of spectral class B9 - A0 ($T_1 \approx 9900 \text{ K}$) and a cooler second component.

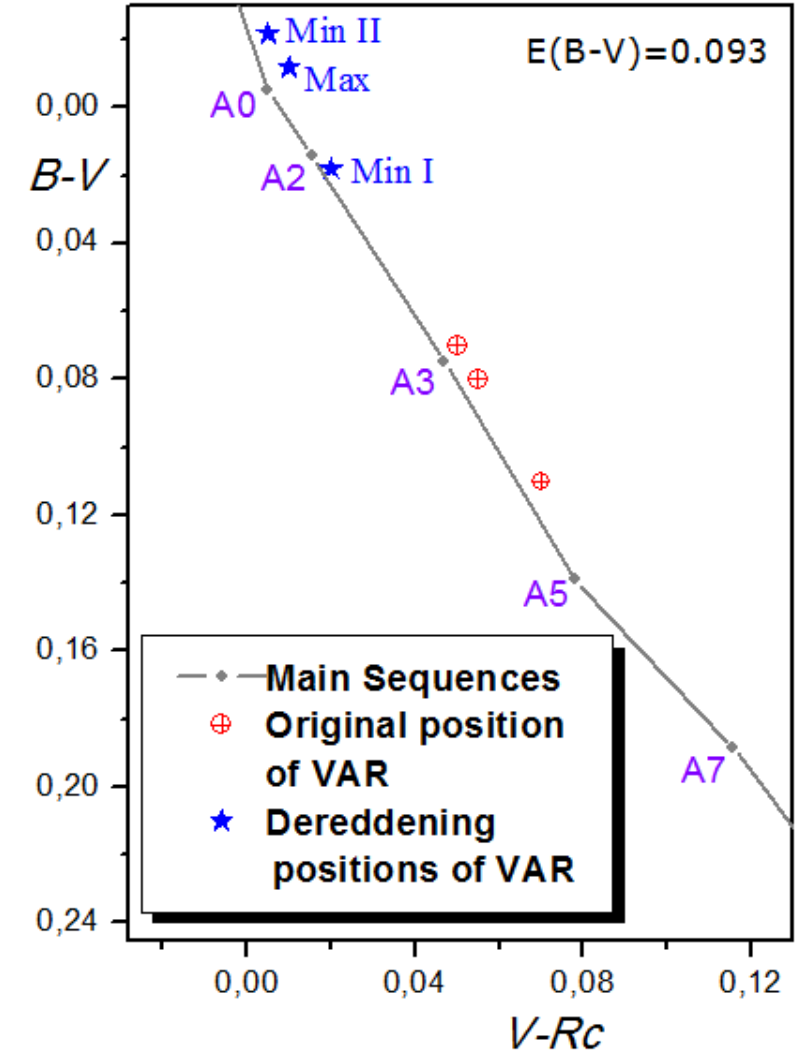
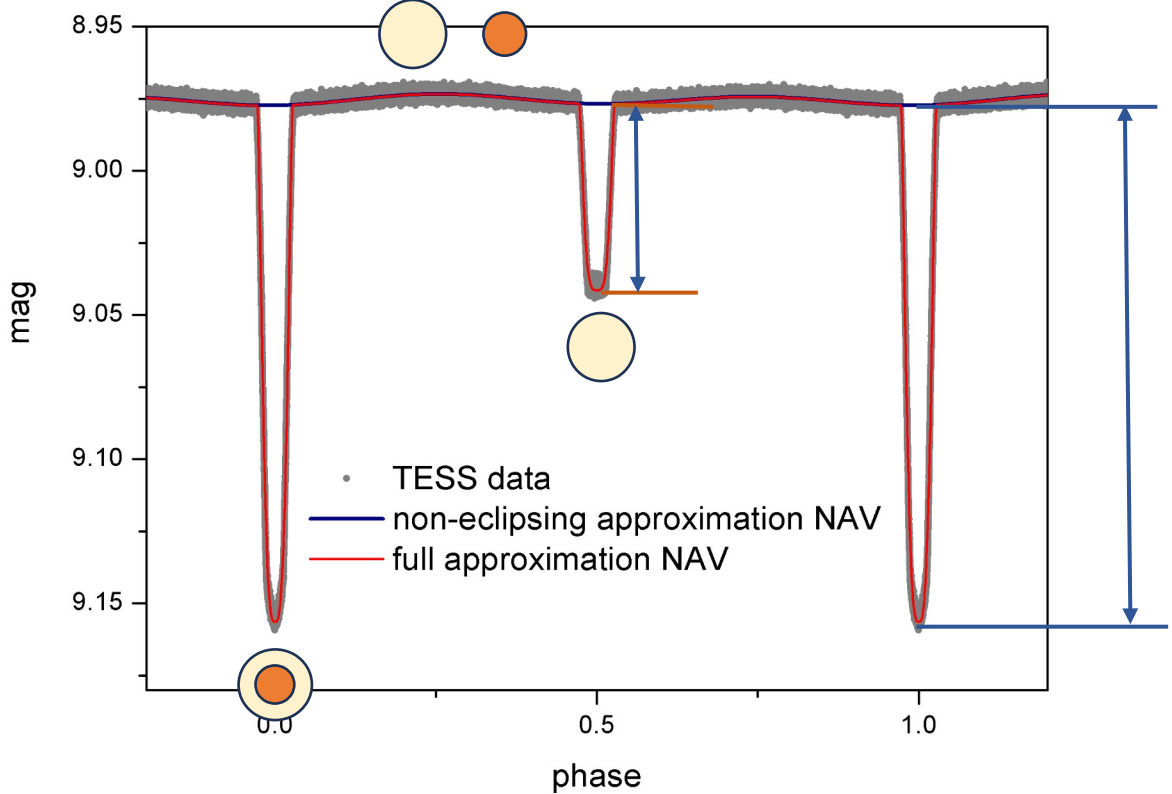


Fig. 10. Our variable's positions in specific phases on two-color diagram.

New Algol Variable (NAV) approximation



Amplitudes of eclipses:
 $\Delta m_1 = 0.1790 \pm 0.0005$
 $\Delta m_2 = 0.0645 \pm 0.0004$



$\Delta m_{ec} = 0.00161 \pm 0.00009$
 $\Delta m_{sp} = 0.0010 \pm 0.0002$

Ellipticity of star(s)

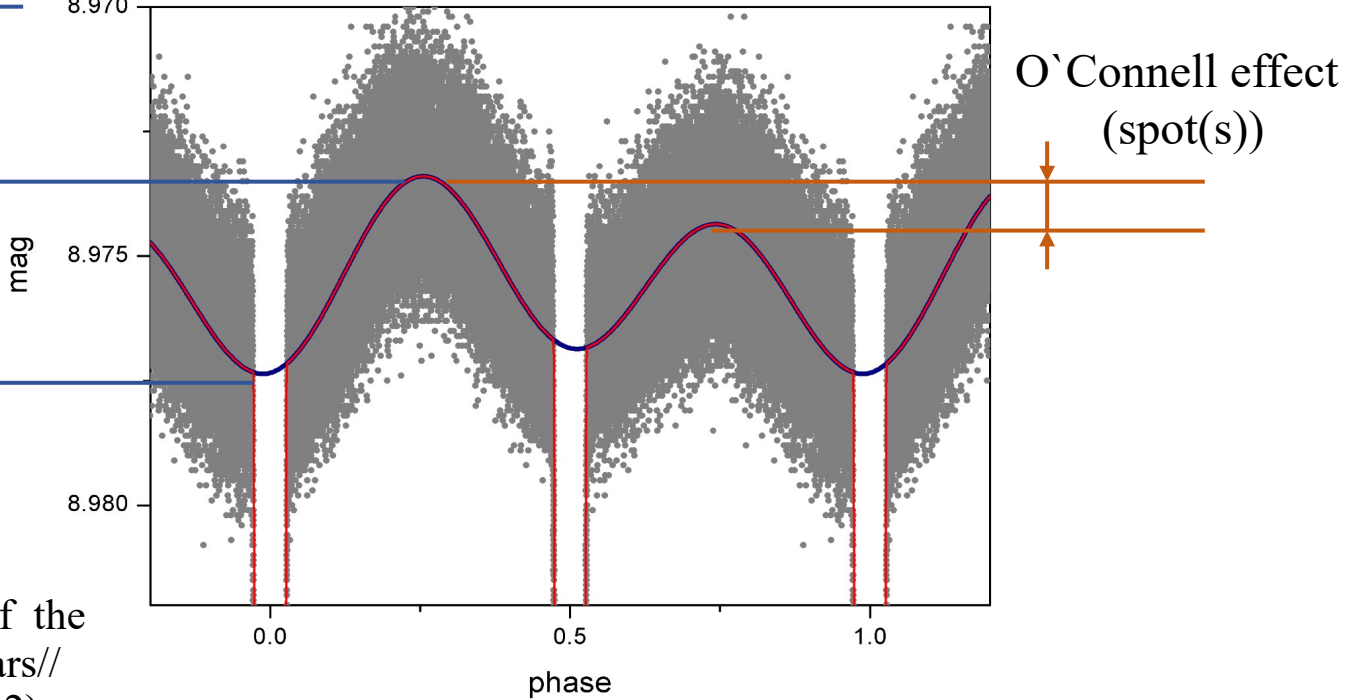


Fig. 11. Amplitudes of eclipses (left) and ellipticity (right).

Andronov, I. L. Phenomenological modeling of the light curves of algol-type eclipsing binary stars// Astrophysics, Volume 55, Issue 4, pp.536-55 (2012)

Estimation of radii ratio and inclination

In terms $L_1+L_2=1$ (non eclipse level),

values of minima depth Δm_1 and $\Delta m_2 \Rightarrow R_2/R_1$

$$\frac{R_2}{R_1} = \sqrt{\frac{1 - 10^{-0.4\Delta m_1}}{10^{-0.4\Delta m_2}}}$$

Phases of inner (ϕ_2) and outer (ϕ_1) discs' contacts $\Rightarrow i$ ($e=0$)

$$i = \arcsin \sqrt{\frac{2\frac{R_2}{R_1}}{\left(1+\frac{R_2}{R_1}\right) \cos^2 2\pi\phi_2 - \left(1-\frac{R_2}{R_1}\right) \cos^2 2\pi\phi_1}}$$

$$\phi_1 = 0.5 - \frac{t_{eclipse}}{2P} \quad \phi_2 = 0.5 - \frac{t_{total\ eclipse}}{2P}$$

Parameter	Value
Δm_1	0.1790 ^m ±0.0005 (NAV)
Δm_2	0.0645 ^m ±0.0004 (NAV)
$t_{eclipse}$	0.3547 ^d (8,51 ^h) ±0.0007 ^d (NAV)
$t_{total\ eclipse}$	0.1717 ^d (4,12 ^h) ±0.0007 ^d (WSL)
Parameter	Value
$\frac{R_2}{R_1}$	0.4015±0.0006
i	89,1275°

Tab. 3. Calculated parameters

RV versus LC

A few days ago we found published radial velocities (2022ApJS..259...35A).

By constructing a curve from this data, folding it with our found orbital period, and superimposing it on our light curve, we can see that the transitions through 0 of the radial velocity curve **exactly** correspond to the main and secondary eclipses.

From the obtained values we found the distance of one component from the center of mass:

$$a_1 = V_1 P / 2\pi \sin i = 0.036 \text{ AU}$$

The sine wave also confirmed circularity of the orbit.

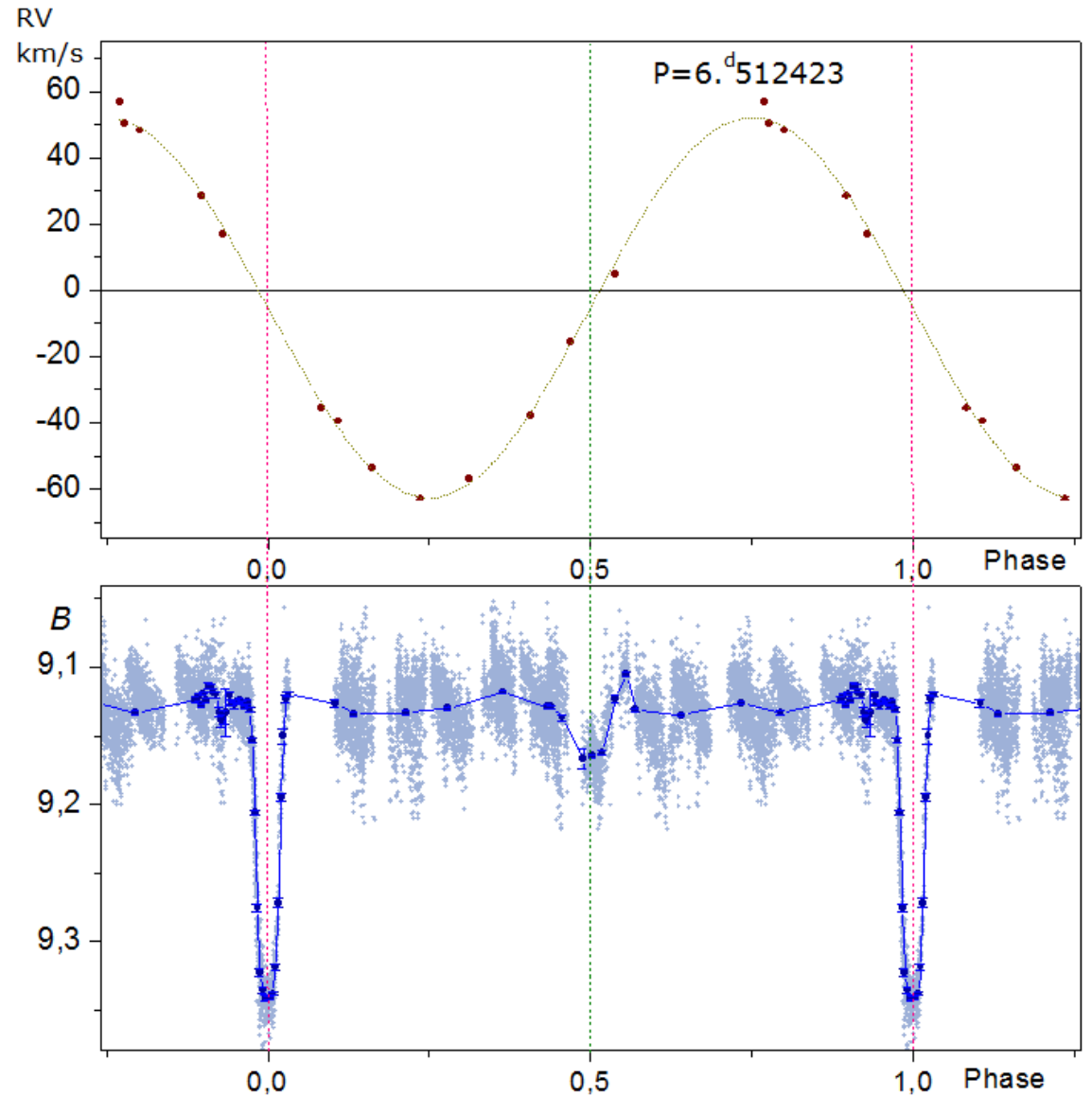


Fig. 12. Phase folded radial velocity curve and light curve.

Conclusions

We discovered variability of the HD 182144 and showed that it belongs to Algol-type eclipsing variables.

As a result of data analysis, we determined:

- orbital period of the system $P = 6.5124230$ d,
- true magnitudes and color indices, spectral class B9 – A0 and temperature of one component of the system $T_1 \approx 9900$ K,
- the radii ratio of the system components $R_2/R_1 = 0.4015$, as well as the orbital inclination $i = 89.13$,
- distance of the first component to the center of mass $a_1 = 0.036$ AU
- circularity of the orbit

Thank you for attention!

Acknowledgement

This research was funded by the EU NextGenerationEU through the Recovery and Resilience Plan for Slovakia under the project No. 09I03-03-V01-00002. We are also grateful for financial support from grants APVV-20-0148, VEGA 2/0030/21 and VEGA 2/0031/22. MV acknowledges the support from the Scholarship of the Slovak Academic Information Agency SAIA.